Journal of Catalysis **210,** 340–353 (2002)
doi:10.1006/jcat.2002.3698

The Influence of Pt Oxide Formation and Pt Dispersion on the Reactions $NO_2 \Leftrightarrow NO + 1/2\ O_2$ over Pt/Al_2O_3 and $Pt/BaO/Al_2O_3$

Louise Olsson[*,†,‡] and Erik Fridell[†,‡,1]

[*]*Department of Chemical Reaction Engineering,* [†]*Competence Centre for Catalysis, and* [‡]*Department of Applied Physics,*
Chalmers University of Technology, SE-412 96 Göteborg, Sweden

Received February 1, 2002; revised May 28, 2002; accepted May 28, 2002

Flow reactor experiments and XPS measurements were used to investigate the observed decrease in activity of Pt/Al_2O_3 and $Pt/BaO/Al_2O_3$ catalysts during reaction conditions. The reactions studied were $NO_{(g)} + 1/2O_{2(g)} \Leftrightarrow NO_{2(g)}$. The influence of platinum dispersion on activity and on the activity decrease with time was also studied. When the Pt/Al_2O_3 catalyst was exposed to NO_2 (350°C), the NO_2 dissociation rate decreased. This activity decrease with time was also studied with XPS and it is suggested that it was due to platinum oxide formation. Further, when the platinum dispersion was increased, the platinum activity decreased and the reason may be that small platinum particles more easily form oxides. According to XPS measurements platinum supported on BaO/Al_2O_3 gave a higher concentration of platinum oxide after NO_2 exposure compared to what was found for Pt supported on only Al_2O_3. Flow reactor experiments also showed that $Pt/BaO/Al_2O_3$ was less active, both for oxidation of NO and for reduction of NO_2, than Pt/Al_2O_3 was and one possible explanation for this is the fact that platinum on BaO/Al_2O_3 forms more oxides.

Key Words: **catalysis; platinum oxide; NO oxidation; NO_2 dissociation; Pt/Al_2O_3; $Pt/BaO/Al_2O_3$; dispersion.**

1. INTRODUCTION

It is of great importance to reduce emissions of the greenhouse gas CO_2 (1). One small contribution in this respect may be obtained by replacing stoichiometric engines with the more-fuel-efficient lean-burn engines. However, a major problem connected to this is the fact that a conventional three-way catalyst is not able to effectively reduce the NO_x emissions in oxygen excess. There are different possible solutions to this problem, e.g., selective catalytic reduction (SCR) with either ammonia or hydrocarbons (HC) (2). The catalysts for HC-SCR can be divided into three groups (2): noble metals, zeolites, and metal oxides. HC-SCR over Pt/Al_2O_3 has been extensively investigated (3–5) and it has been suggested that when the hydrocarbon is an alkane, a crucial step is to oxidize NO to NO_2 over noble metal sites. This NO_2 then reacts with HC on the support to form N_2.

A different approach is the NO_x storage concept, where NO_x is trapped in the catalyst during lean conditions and released during short rich excursions obtained by engine control (6–12). In the NO_x storage concept the catalysts contain a storage material, e.g., BaO, noble metals like Pt and Rh, alumina, and other additives. The mechanism for NO_x storage has been investigated both experimentally (6, 8–9), with microkinetic modeling (10), and using first-principal calculations based on the density functional theory (13). During the lean period NO is first oxidized over Pt sites to form NO_2, which is stored, by forming compounds with barium. During the short rich periods NO_x desorbs from the storage sites and reacts with the hydrocarbons over the noble metals to form N_2, CO_2, and H_2O.

It is thus well established that the oxidation of NO to NO_2 over Pt is an important step for both NO_x storage and HC-SCR (at least with alkanes). NO oxidation on supported platinum has been investigated previously, in experiments with only NO and O_2 as reactants (14, 15), in experiments with SO_2 added to the feed (16), and in experiments under lean-burn conditions with hydrocarbons present (17, 18). It has been found that Pt particle size influences the NO oxidation rate (15), suggesting that the reaction is structure sensitive (16). When the dispersion is decreased, giving larger particles, the oxidation capacity of platinum increases (15, 16, 18). This was found for Pt supported both on SiO_2 (18) and on Al_2O_3 (15, 18). Denton *et al.* (18) investigated the difference between Pt/SiO_2 and Pt/Al_2O_3 and they concluded that the dispersion is a key parameter and the effect of the support (silica or alumina) was not easily distinguishable. However, according to Xue *et al.* (16) particle size is very important for Pt/SiO_2, but the effect is much less significant for Pt/Al_2O_3.

Another feature that may influence the activity of platinum is oxide formation. Platinum oxides have been investigated with several experimental techniques: X-ray photo electron spectroscopy (XPS) (19–22), X-ray absorption spectroscopy (EXAFS (23) and XANES (24)), temperature-programmed reduction (TPR) (25),

---

[1] To whom correspondence should be addressed. Fax: +46-31-772 3134. E-mail: fridell@fy.chalmers.se.

0021-9517/02 $35.00

thermogravimetry–differential scanning calometry (TG–DSC) (26, 27), and low-energy ion scattering (IS) (28). Many of the experimental studies were focused on identifying oxides after a certain pretreatment of the catalyst, such as exposure to O_2 (25–28), O_3 (29), or NO (19). Yazawa *et al.* (30) investigated the long-term change in activity due to oxide formation in a propane–oxygen mixture for Pt/SiO_2–Al_2O_3 and Pt/ZrO_2 catalysts. Also, during CO oxidation, platinum oxide formation has been observed (31–34). Most authors claim, especially for low-pressure experiments, that CO reconstructs the surface (31, 32) and after that oxides or subsurface oxygen can be formed.

Further, the acidity/alkalinity of the support seems to influence the formation of platinum oxides (24, 30). If the support is acidic, the formation of platinum oxides is suppressed. There are different suggestions as to how the support influences the noble metal particles. According to Yoshida *et al.* (24) an acidic support is electrophilic and the 5d band in platinum donates electron density to the support. When platinum oxide is formed electrons are transferred from Pt to oxygen, and in the case of an acidic support there is a lower electron density in Pt and this suppress the formation of oxides (24).

In the present study we investigate the reversible reaction NO oxidation to NO_2 and NO_2 dissociation to NO. Flow reactor experiments are used to monitor the transient activity decrease of the catalyst under reaction conditions. XPS experiments are used to monitor the suggested formation of PtO and PtO_2. Further, a comparison of the oxide formation for Pt supported on Al_2O_3 and on BaO/Al_2O_3 is made, which indicates increased amounts of oxides when the NO_x storage material BaO is present.

2. EXPERIMENTAL

In this study Pt/Al_2O_3 and $Pt/BaO/Al_2O_3$ monolith catalysts were used for flow reactor experiments and XPS measurements. The weight of the washcoat and the amount of Pt and BaO in the catalysts are given in Table 1. The monoliths consist of 188 channels ($\approx 1 \times 1$ mm) and the length of the samples are shown in Table 1. The catalyst preparation procedure is described elsewhere (8, 35). Briefly, cordierite was first impregnated with alumina and calcined at 600°C for 2 h. For the samples containing BaO the alumina washcoat was impregnated with $Ba(NO_3)_2$ and calcined at 600°C for 2 h. Finally, Pt was added to the catalysts by wet impregnation using a platinum(II) nitrate solution, which was prepared by diluting a 15.35 wt% $Pt(NO_3)_2$ solution from Heraeus with distilled water. Sample 1 (C1) was then calcined at 600°C for 2 h, while C2 and C3 were calcined at 400°C for 3 h. The fresh catalysts were treated in hydrogen for 30 min (C2 and C3, 4% H_2/Ar at 400°C; C1, 2% H_2/Ar at 500°C). The lower calcination temperature for C2 and C3 was chosen in order to get a higher dispersion.

TABLE 1

Composition, Weight, and Length of Catalyst Samples

Sample	Weight of washcoat (mg)	Wt% Pt (of washcoat)	Wt% BaO (of washcoat)	Monolith length (mm)
C1	579	1.9	—	15
C2	423	1.9	—	10
C3	418	1.9	15	10
C4 (XPS)	—	2.7	—	—
C5 (XPS)	—	3.0	13	—

In this study two different flow reactors were used. One was used for CO- and O_2-TPD experiments and the other for the NO_x experiments. The main principle for the two setups was similar. The catalyst was placed in a quartz tube with a thermocouple about 1 cm in front of the catalyst (with respect to the gas flow) and for the TPD experiments there was a second thermocouple inside the sample. The gas flow into the reactors was controlled by mass flow controllers. The detection of the gas products differed between the two setups. In the reactor used for TPD experiments a mass spectrometer (Balzer QME 125) was used to measure CO, CO_2, and O_2 concentrations. In the other setup a chemiluminescense detector (CLD 700) was used to monitor the NO and NO_2 concentrations. The pressure in both reactors was 1 atm and the inert balance was Ar. The total flow for the second setup (with the NO_x detector) was 3000 ml/min.

The dispersion of Pt was measured by CO-TPD experiments and the CO/Pt ratio is presented. The catalysts were pretreated (400°C for C2 and C3, 450°C for C1) with 1% O_2/Ar for 10 min to remove all hydrocarbon species and after another 5 min in Ar the samples were reduced in 4% H_2. The temperature was then decreased to 5°C in the same H_2/Ar flow. After another 5 min in Ar the catalyst was exposed to 2000 ppm CO for 10 min, followed by 15 min of inert flow at 5°C and then a temperature ramp with a speed of 40°C/min to 450°C for C2 and C3, 500°C for C1. The Ar flow during the temperature ramp was 50 ml/min. The reason for the lower pretreatment temperature for C2 and C3 is that it was crucial not to sinter the samples during the CO-TPD experiments.

The final dispersion for catalysts C2 and C3 was also measured with hydrogen chemisorption, with the use of a chemisorption instrument (Micromeritics ASAP 2010). The catalysts were pretreated with oxygen for 30 min at 350°C, followed by hydrogen for 120 min at 400°C. The reactor was outgassed and the sample cooled to 35°C, where hydrogen was dosed on the sample. Finally, the reactor was outgassed and exposed to hydrogen again. The amount of chemisorbed hydrogen was taken as the difference between the two hydrogen exposures.

The oxygen-TPD experiments were performed on catalyst C1. First the sample was heated to 700°C in Ar and then pretreated with 4% H_2/Ar at 500°C. The temperature was then decreased to 350°C and the catalyst was exposed to different amounts of oxygen. In the first experiment the exposure was 200 ppm O_2/Ar for 5 min, in the second experiment it was 8% O_2/Ar for 5 min, and in the final experiment it was 8% O_2/Ar for 4 h and 30 min. After the oxygen exposure, the temperature was rapidly decreased with the same O_2/Ar flow over the sample in order to avoid desorption of O_2. When the temperature was below 150°C (where O_2 desorption is negligible) the flow was changed to Ar as the temperature decreased to room temperature. The system was vacuum pumped to remove all residuals of O_2 in the feed gas and then a temperature ramp (40°C/min) was conducted with a flow of 50 ml Ar/min to 700°C.

The influence of the Pt dispersion on the NO oxidation and NO_2 dissociation to NO was investigated both for the Pt/Al_2O_3 (C2) and for the $Pt/BaO/Al_2O_3$ (C3) catalyst. The following experimental sequence was used for this investigation:

1. CO-TPD to determine the CO/Pt ratio, i.e., to get the number of surface platinum sites.
2. NO_2 dissociation experiment at 350°C.
3. NO oxidation experiment, temperature ramp.
4. Sintering of the sample for 45 min in Ar.

These four steps were repeated four times, with increasing sintering temperatures from 550 to 650°C and finally to 750°C. Prior to each experiment (NO oxidation, NO_2 dissociation, or sintering) the catalyst was pretreated at 400°C for 10 min in 0.1% H_2/Ar followed by 10 min in Ar. For the NO_2 dissociation experiments the temperature was decreased to 350°C and the catalyst was exposed to 630 ppm NO_2/Ar for 90 min. In the NO oxidation experiments the catalyst was exposed to 620 ppm NO, 8% O_2/Ar at room temperature for 35 min followed by a temperature ramp to 400°C, with a speed of 5°C/min.

The decomposition of NO_2 to NO was investigated at different temperatures (300, 350, and 400°C) for catalyst C2. Catalyst C1 was used to make mechanistic experiments of the deactivation: A NO_2 dissociation experiment with 630 ppm NO_2/Ar at 350°C for 3 h was performed after heating the catalyst to 700°C in Ar. A steady-state experiment with NO/O_2 was also performed, where the catalyst was exposed to 620 ppm NO, 8% O_2/Ar for 3 h at 250°C, followed by 3 h at 300°C. Further, an experiment at 350°C was performed for 20 min in 630 ppm NO_2/Ar, followed by 60 min in 8% O_2/Ar and 10 min in 630 ppm NO_2. In the final mechanistic experiment the catalyst was exposed to 630 ppm NO_2/Ar at 350°C for 60 min and cooled to 90°C in the same gas flow; at 90°C it was flushed with Ar for 60 min, followed by exposure to 630 ppm NO_2/Ar. After 2 min the temperature was raised to 350°C with the same gas flow over the sample and at this temperature the gas composition was altered as follows: 10 min in 630 ppm NO_2/Ar; 5 min in Ar; 5 min in 630 ppm NO_2/Ar; 5 min in Ar; 10 min in 620 ppm NO, 8% O_2/Ar; 5 min in Ar; 5 min in 630 ppm NO_2/Ar, Ar. The pretreatment for the last three experiments was 15–20 min in 0.1 or 0.6% H_2/Ar at 500°C, followed by 15 min in Ar at 600°C.

The XPS study was undertaken using a Perkin–Elmer PHI 5000 C system, at a pressure of $<10^{-9}$ mbar, equipped with a pretreatment cell allowing the samples to be exposed to various gas mixtures at 1 atm and transferred to the UHV chamber without being exposed to ambient air. The analysis was performed for catalysts C4 (Pt/Al_2O_3) and C5 ($Pt/BaO/Al_2O_3$) after different pretreatments. The samples were initially oxidized in 19% O_2 at 500°C for 10 min in order to remove adsorbed hydrocarbons and then reduced in 8% H_2 at 500°C for 15 min. The samples were then cooled in vacuum, transferred to the UHV chamber, and analyzed. After this the samples were returned to the pretreatment cell and exposed to 700 ppm NO_2 at 350°C for 90 min, cooled in NO_2 to 140°C, and then analyzed again. Finally the samples were reduced in 8% H_2 at 500°C for 60 min, oxidized in 19% O_2 at 400°C for 60 min, cooled in O_2 to 50°C, and again analyzed. The XPS spectra were recorded using nonmonochromatic Al $K\alpha$ radiation. Electrons originating from a spot with a diameter of 800 μm were collected. The energy scale was calibrated by setting the Al 2s peak at 119.3 eV (36). The FWHM for this peak was between 2.9 and 3.2 eV for all measurements. The calibration produced O 1s peaks at 531.0 ± 0.2 for the $Pt/BaO/Al_2O_3$ sample and at 531.3 ± 0.1 for the Pt/Al_2O_3 sample for all pretreatments. Charge compensation by a flood gun was not used since this was not found to improve the shape of the peaks. The X-ray power was 400 W and the pass energy for the analysis of Pt 4f was 5.85 eV for all measurements. For this region 10 sweeps were overlapped, taken with 0.025 eV/step and 100 ms/step. The spectra for the Pt 4f region were used to obtain the relative abundance of different Pt species. This was obtained from curve fitting using the Perkin–Elmer MultiPak software. To do this we subtracted the contribution from the Al 2p peak at 74.3 eV. The area and position of this peak was obtained by comparing it with the Al 2s peak. The data was then fitted to the Pt 4f doublet for Pt, PtO, and PtO_2 using the following restrictions (21): The doublet separation was set to 3.3 eV for all three compounds, and the $4f_{7/2} : 4f_{5/2}$ area ratio was set to 1.3, 1.39, and 1.48 for Pt, PtO, and PtO_2, respectively.

3. RESULTS

3.1. Flow Reactor Studies: NO Oxidation/NO_2 Dissociation on Pt/Al_2O_3

The outlet concentrations of NO, NO_2, and NO_x during a 3-h exposure to 630 ppm NO_2/Ar over a Pt/Al_2O_3 catalyst (C1) at 350°C are shown in Fig. 1. The activity of Pt for dissociation of NO_2 to NO gradually decreases during the experiment and the concentration of NO goes from 465 to

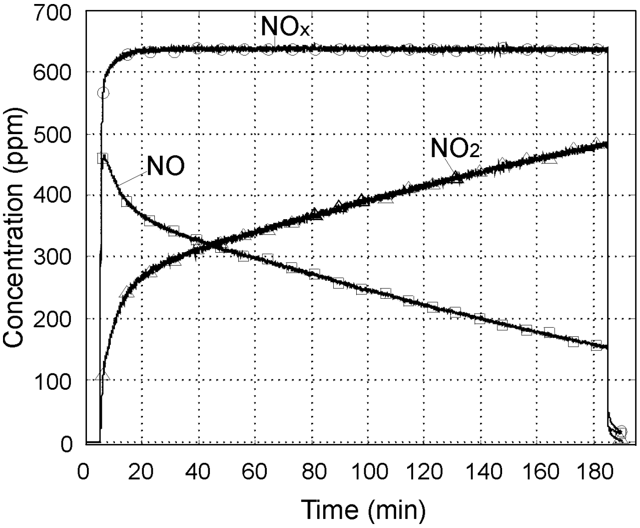

FIG. 1. Measured NO (squares), NO_2 (triangles), and NO_x (circles) outlet concentrations when exposing a Pt/Al_2O_3 catalyst (C1) to 630 ppm NO_2 in Ar for 180 min at 350°C.

155 ppm during the 3-h experiment. During the first 20 min some NO_x is stored on the catalyst, which is manifested by the NO_x signal slowly approaching its steady-state level. After the first 20 min the NO_x level is constant. The temperature dependence of this activity decrease with time of platinum is shown in Fig. 2. In this figure the NO and NO_x concentrations are shown after a 90-min exposure to 630 ppm NO_2/Ar on a Pt/Al_2O_3 catalyst (C2) at temperatures of 300, 350, and 400°C. All three experiments show that the Pt activity decreases. However, the experimental accuracy for observing the deactivation of platinum is best at 350°C. This is the reason for conducting the mechanistic experiments at this temperature. It should be pointed out that at higher temperature the concentrations are closer to their equilibrium values and the conversion is not likely to be as strongly influenced by a decrease in the number of active sites. Further, the long-term activity for oxidation of NO to NO_2 was also investigated for catalyst C1 (Pt/Al_2O_3). In this experiment, the catalyst was exposed to 620 ppm NO, 8% O_2/Ar for 3 h at 250°C, followed by 3 h at 300°C. The resulting NO, NO_2, NO_x concentrations and the temperature from this experiment are shown in Fig. 3. In this experiment the activity of platinum also decreases with time, resulting in a slow decrease in the NO_2 concentration. The negative slope in the NO_2 concentration is larger at 250 than at 300°C.

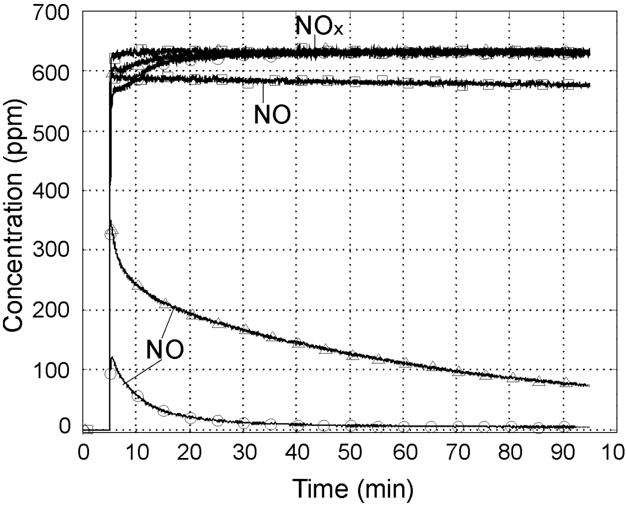

FIG. 2. Measured NO and NO_x outlet concentrations when exposing a Pt/Al_2O_3 catalyst (C2) to 630 ppm NO_2 in Ar for 90 min at 300°C (circles), 350°C (triangles), and 400°C (squares).

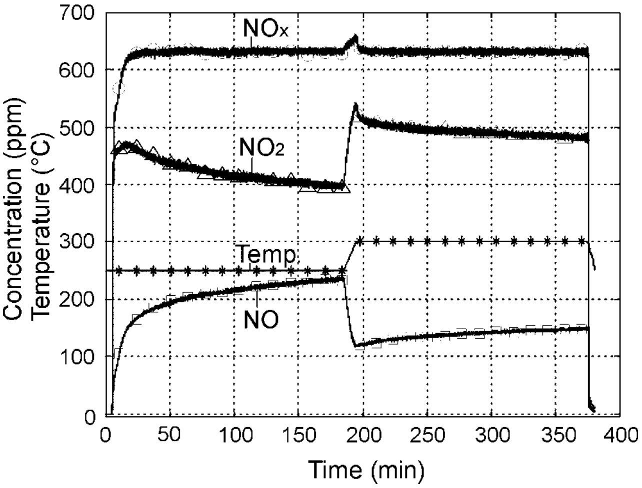

FIG. 3. Measured NO (squares), NO_2 (triangles), and NO_x (circles) outlet concentrations and inlet gas temperature when exposing a Pt/Al_2O_3 catalyst (C1) to 620 ppm NO, 8% O_2/Ar for 180 min at 250°C and 180 min at 300°C.

The influence of the dispersion on the NO_2 dissociation and NO oxidation capacity of platinum was investigated. To eliminate the risk that differences seen in experiments may be influenced by the fact that two catalysts are never perfectly identical, we chose to use only one catalyst (C2) and to change the dispersion by intermediate treatments at different temperatures. The sequence used is described under Experimental. The results from the CO-TPD experiments are given in Table 2. It should be mentioned that

TABLE 2

CO/Pt and H/Pt Molar Ratios after Exposure at 5 and 35°C, Respectively, for Catalyst C2 (Pt/Al_2O_3) Following Pretreatment in Ar at Increasing Temperatures

Pretreatment temperature (°C)	CO/Pt	H/Pt
400	0.07	n.d.[a]
550	0.06	n.d.
650	0.04	n.d.
750	0.02	0.04

[a] n.d., Not detected.

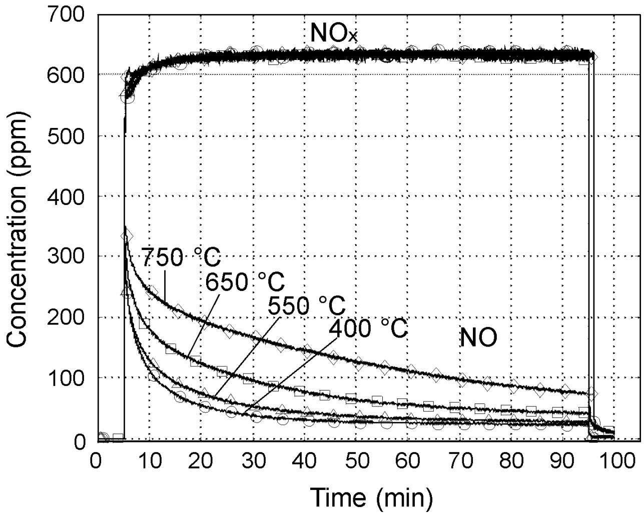

FIG. 4. Measured NO and NO_x outlet concentrations when exposing a Pt/Al_2O_3 catalyst (C2) to 630 ppm NO_2 in Ar for 90 min at 350°C for four different levels of sintering. The pretreatment temperatures were 400°C (circles), 550°C (triangles), 650°C (squares), and 750°C (diamonds).

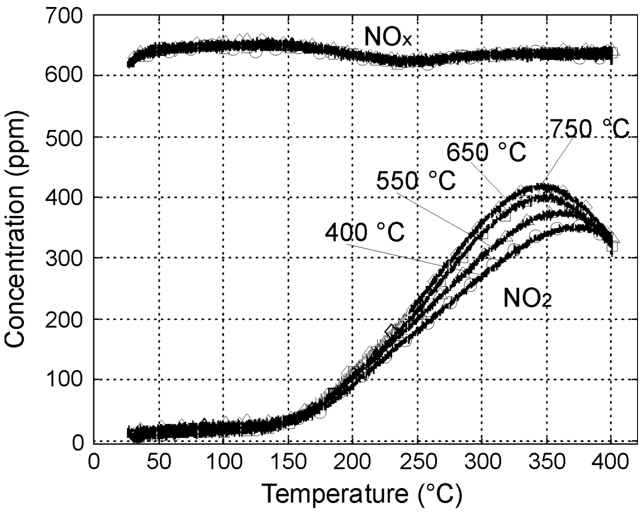

FIG. 5. Measured NO_2 and NO_x outlet concentrations when exposing a Pt/Al_2O_3 catalyst (C2) to 620 ppm NO, 8% O_2/Ar for 35 min, followed by a temperature ramp for four different levels of sintering. The pretreatment temperatures were 400°C (circles), 550°C (triangles), 650°C (squares), and 750°C (diamonds).

prior to the experiment with a pretreatment temperature of 400°C, the catalyst had been heated rapidly to 450°C during another CO-TPD experiment. Further, the result from a hydrogen chemisorption experiment after the last pretreatment (at 750°C) is also given. According to the results shown in Table 2, the dispersion is decreased as the pretreatment temperature is increased, which is expected. The value of H/Pt is somewhat higher than that of CO/Pt after the last pretreatment. This is discussed further under Discussion. The change in activity with increasing pretreatment temperature can be seen in Fig. 4, showing the NO and NO_x concentrations during NO_2 dissociation experiments. The different pretreatment temperatures of the catalyst prior to each experiment are given in the figure. The dissociation of NO_2 to NO decreases during all experiments, due to deactivation of platinum, in the same way as shown in Fig. 1. The initial deactivation rates are given in Table 3. For the catalyst with high dispersion, the conversion of NO_2 to NO and O_2 was low, and as the dispersion decreased the conversion gradually increased and showed its highest value for the catalyst with only 0.02 in CO/Pt ratio. The dependence of the NO oxidation on the different pretreatment temperatures is shown in Fig. 5, where the NO_2 and NO_x concentrations are plotted from the four experiments. As the temperature is increased to about 350°C the conversion of NO to NO_2 is increased. Up to this temperature the conversion is kinetically determined (14). At higher temperatures the conversion starts to decrease, because here the conversion is determined by the thermodynamic concentrations in the equilibrium reaction $NO_{(g)} + 1/2\,O_{2(g)} \Leftrightarrow NO_{2(g)}$. Further, when the dispersion decreases, the oxidation of NO to NO_2 increases. Both the low-temperature activity and the maximum conversion increase as the catalyst becomes more sintered. This is also shown in Table 4, where the temperature at which 50% conversion is first obtained and the maximum NO_2 concentration are shown. The NO_x concentration curves show that initially there is a small contribution from desorption of NO_x that was stored

TABLE 3

The Initial Deactivation Rate for Catalyst C2 (Pt/Al_2O_3) during NO_2 Dissociation Experiments Following Increasing Pretreatment Temperature in Ar

Pretreatment temperature (°C)	Initial deactivation rate (μmol/s/g washcoat)
400	27
550	24
650	21
750	14

TABLE 4

Temperature of 50% Conversion and Maximum NO_2 Concentration after Temperature Ramps with 600 ppm NO and 8% O_2 over C2 (Pt/Al_2O_3) for Different Dispersions[a]

CO/Pt ratio	Temperature of 50% conversion (°C)	Maximum NO_2 concentration (ppm)
0.07	330	350
0.06	309	375
0.04	290	400
0.02	283	420

[a] Given as the CO/Pt ratio obtained in the CO-TPD experiments.

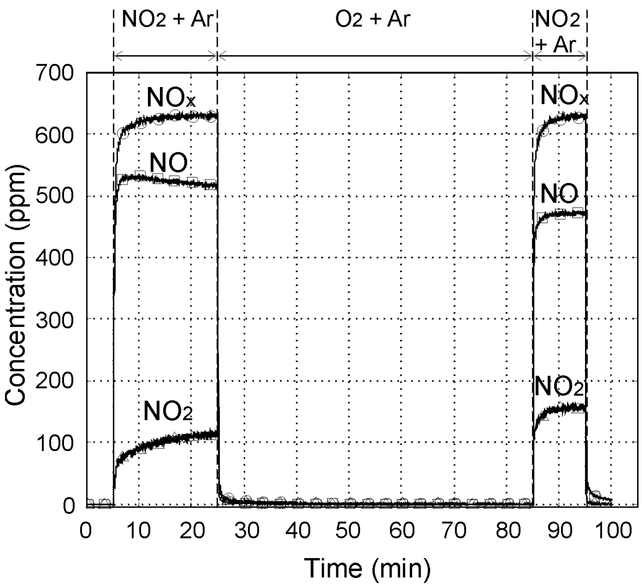

FIG. 6. Measured NO (squares), NO_2 (triangles), and NO_x (circles) outlet concentrations when exposing a Pt/Al_2O_3 catalyst (C1) to 630 ppm NO_2/Ar for 20 min, followed by 8% O_2/Ar for 60 min and 630 ppm NO_2/Ar for 10 min. The temperature in the experiment was 350°C.

in the catalyst during the exposure of NO and O_2 at room temperature, and there is also a small desorption at higher temperatures.

From the results shown in Figs. 1 and 4 it is clear that during NO_2 exposure platinum is deactivated. Therefore, we also investigated whether oxygen, which is a milder oxidizing agent, has the same deactivating effect. An experiment at 350°C was performed with catalyst C1 (Pt/Al_2O_3), where the sample was exposed to 20 min of 630 ppm NO_2/Ar, followed by 60 min of 8% O_2/Ar and finally 10 min of 630 ppm NO_2/Ar. The outlet concentrations of NO, NO_2, and NO_x from this experiment are shown in Fig. 6. During the first 20 min of NO_2 exposure the NO concentration slowly decreases. After the oxygen exposure the conversion of NO_2 to NO is lower than it was prior to the oxygen treatment.

To try to resolve more of the features of the activity decrease with time another experiment was performed with catalyst C1 (Pt/Al_2O_3), as described under Experimental. The results are shown in Fig. 7, where the concentrations of NO, NO_2, and NO_x as well as the temperature (dash–dotted line) are shown. The inlet gases during the different periods are also given in this figure. During the first NO_2 exposure at 350°C the NO concentration can be seen to decrease with time, in the same way as is shown in previous figures. The temperature is then decreased to 90°C with the same gas mixture (NO_2/Ar) and during this period an uptake of NO_x is seen. The catalyst is then flushed with Ar and some desorption of NO_x occurs. After the NO_2 is switched on the concentration goes up slowly, because NO_x is again being stored on the catalyst. When the temperature is raised, NO_x desorbs rapidly and a large NO_x peek is seen. It should be mentioned that the NO_x peak is actually even larger than what is seen in the figure, since the NO_x concentration was so high that the NO_x detector got out of range. At 350°C almost no conversion of NO_2 is seen (only 16 ppm NO). This is very different from what was observed before the cooling in NO_2/Ar, where 365 ppm NO was formed. After flushing the catalyst with Ar for 5 min at 350°C the catalyst is again exposed to NO_2/Ar and it can be seen that it has regained some of its activity for dissociating NO_2 to NO, so that 23 ppm NO now is formed. Again the catalyst is flushed with Ar for 5 min followed by exposure to a gas mixture containing 630 ppm NO and 8% O_2/Ar for 10 min. The catalyst is found to be active for oxidizing NO to NO_2 and about 360 ppm NO_2 is formed. During these 10 min of $NO + O_2$ exposure the activity of the catalyst gradually increases and after 10 min the concentration of NO_2 goes up to 380 ppm. After this the catalyst is flushed with Ar for 5 min and NO_2/Ar is introduced again. Now the catalyst is able to dissociate NO_2 to NO again and initially 330 ppm NO is formed. During these 5 min of NO_2 exposure the activity decreases again and this time more rapidly.

Figure 6 shows that also O_2 in Ar causes activity decrease in the platinum catalyst. Three O_2-TPD experiments were therefore performed to investigate how the exposure time and concentration of O_2 influence the amount of oxygen on the Pt/Al_2O_3 catalyst (C1). After a pretreatment which consisted of heating the catalyst to 700°C in Ar followed by

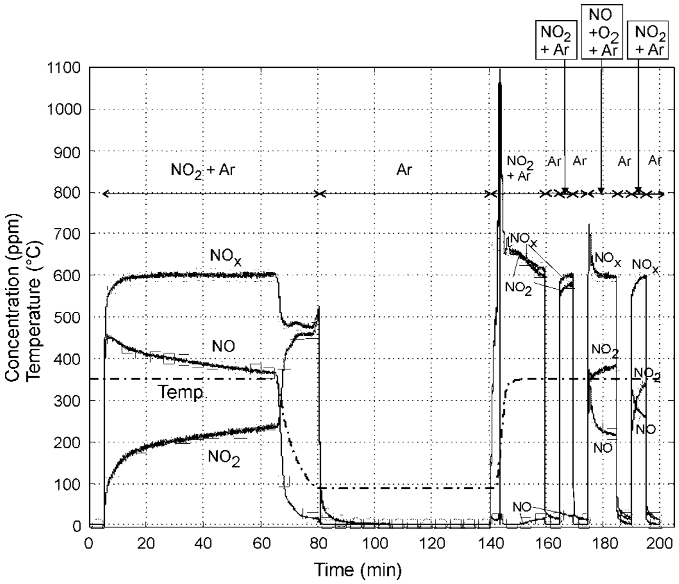

FIG. 7. Measured NO (squares), NO_2 (triangles), and NO_x (circles) outlet concentrations after an experiment with a Pt/Al_2O_3 catalyst (C1). The inlet gas mixture and temperature varied as follows: 630 ppm NO_2/Ar for 60 min at 350°C, cooled to 90°C; Ar for 60 min at 90°C; 630 ppm NO_2/Ar for 2 min at 90°C; heating to 350°C in 630 ppm NO_2/Ar; and at 350°C, 630 ppm NO_2/Ar for 10 min, Ar for 5 min, 630 ppm NO_2/Ar for 5 min, Ar for 5 min, 620 ppm NO with 8% O_2/Ar for 10 min, Ar for 5 min, 630 ppm NO_2/Ar for 5 min, Ar.

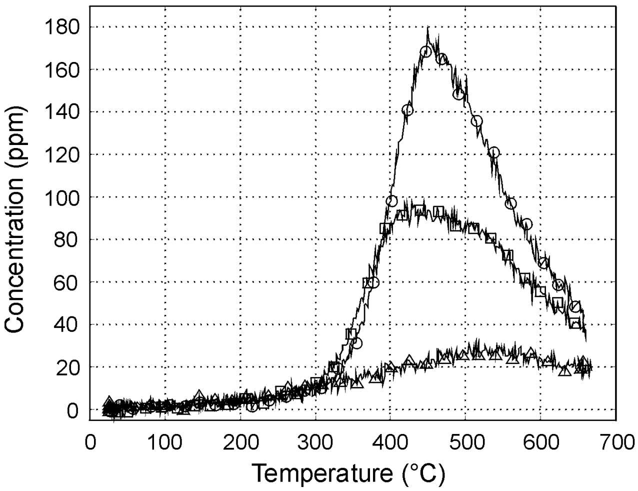

FIG. 8. Oxygen-TPD for a Pt/Al_2O_3 catalyst (C1). Prior to the temperature ramp the catalyst was exposed to either 200 ppm O_2/Ar for 5 min (triangles), 8% O_2/Ar for 5 min (squares), or 8% O_2/Ar for 4 h and 30 min (circles) at 350°C.

H_2/Ar at 500°C, the catalyst was exposed to either 200 ppm O_2 for 5 min, 8% O_2 for 5 min, or 8% O_2 for 4 h and 30 min at 350°C. After the pretreatment the catalyst was heated in Ar from room temperature to 700°C, at a speed of 40°C/min. The results from the three TPD experiments are shown in Fig. 8. At about 300°C the desorption of O_2 starts and the maximum desorption is obtained at approximately 450°C. There is a large difference between the three experiments: When the catalyst is exposed to a low concentration of O_2 for a short period (5 min) there is only a small amount of oxygen adsorbed on the surface. In the second experiment the oxygen exposure time is the same but the concentration is increased by a factor of 400 and the amount of oxygen adsorbed on the catalyst increases substantially. In the final experiment with both a high concentration and a long exposure time (4 h and 30 min) the maximum peak increases even more. The amount of oxygen desorbing from the catalyst was integrated and the ratio of the surface platinum sites that was covered with oxygen atoms, compared with CO adsorption from CO-TPD, is given in Table 5. In the first experiment, the oxygen/CO ratio was about 1; however, for the other two experiments the ratio was well above 1.

TABLE 5

Ratio of Oxygen-Covered Pt Sites during O_2-TPD Experiments after Three Different Pretreatments[a] in Relation to CO-Covered Pt Sites during CO-TPD

O_2 concentration	Time for O_2 exposure	Oxygen/CO ratio
200 ppm	5 min	1.0
8.1%	5 min	1.6
8.1%	4 h 30 min	2.4

[a] O_2 concentration and time of O_2 exposure were varied.

TABLE 6

CO/Pt and H/Pt Molar Ratios after Exposure at 5 and 35°C, Respectively, for Catalyst C3 ($Pt/BaO/Al_2O_3$) Following Pretreatment in Ar at Increasing Temperatures

Pretreatment temperature (°C)	CO/Pt	H/Pt
400	0.010	n.d.[a]
550	0.008	n.d.
650	0.006	n.d.
750	0.007	0.02

[a] n.d., Not detected.

3.2. *Flow Reactor Studies: NO Oxidation/NO_2 Dissociation on $Pt/BaO/Al_2O_3$*

The influence of the dispersion on the NO_2 dissociation and NO oxidation capacity of $Pt/BaO/Al_2O_3$ (C3) was investigated in the same way as for the Pt/Al_2O_3 catalyst, described in the previous section. The CO/Pt ratio was measured with CO-TPD and then a NO_2 dissociation experiment was performed with 630 ppm NO_2/Ar for 90 min at 350°C, followed by a NO oxidation experiment, where the temperature was increased by 5°C/min with 620 ppm NO, 8% O_2/Ar in the gas flow. The catalyst was then sintered at 550, 650, or 750°C and the same procedure was repeated. In Table 6 the CO/Pt ratio from the CO-TPD measurements are shown. It was found to be about 0.01 in all cases. Further, the result from an hydrogen chemisorption experiment after the last pretreatment (at 750°C) is also given. Figure 9 shows the NO and NO_x concentrations from the NO_2 dissociation experiments. The curves are labeled with the sintering temperature. The amount of NO produced

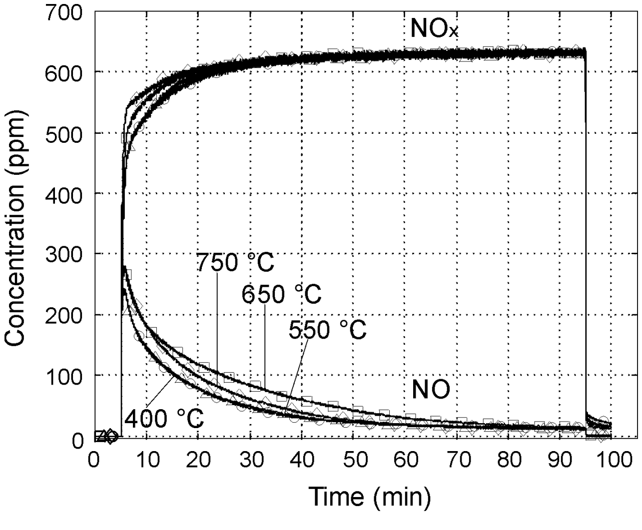

FIG. 9. Measured NO and NO_x outlet concentrations when exposing a $Pt/BaO/Al_2O_3$ catalyst (C3) to 630 ppm NO_2 in Ar for 90 min at 350°C after four different pretreatments. The pretreatment temperatures were 400°C (circles), 550°C (triangles), 650°C (squares), and 750°C (diamonds).

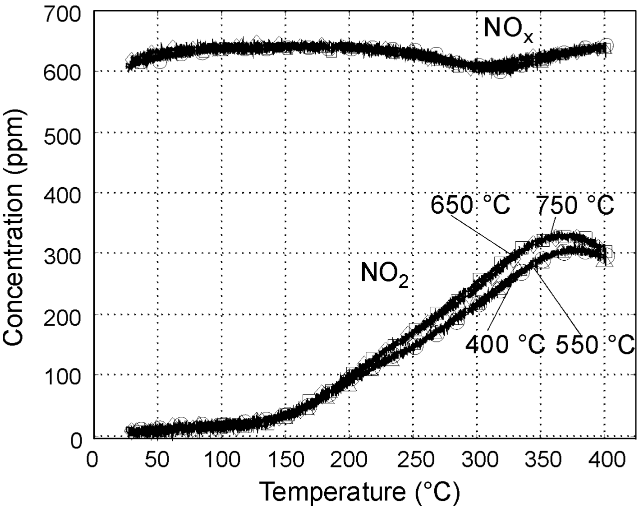

FIG. 10. Measured NO$_2$ and NO$_x$ outlet concentrations when exposing a Pt/BaO/Al$_2$O$_3$ catalyst (C3) to 620 ppm NO, 8% O$_2$/Ar for 35 min, followed by a temperature ramp after four different pretreatments. The pretreatment temperatures were 400°C (circles), 550°C (triangles), 650°C (squares), and 750°C (diamonds).

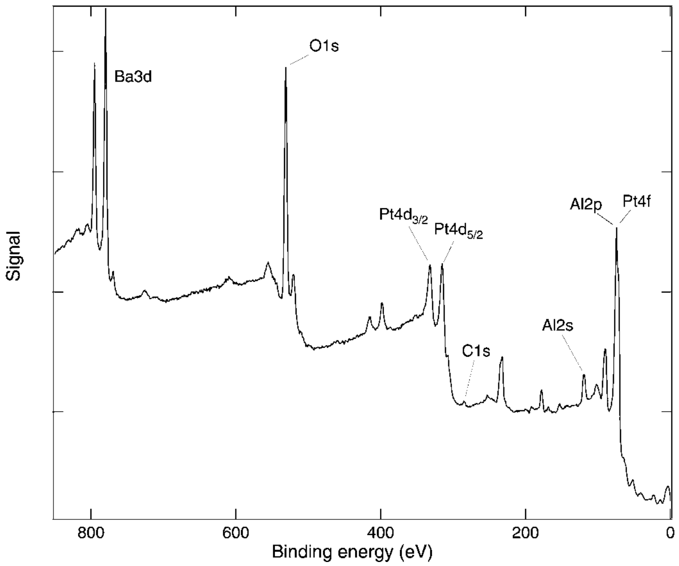

FIG. 11. An overview spectrum for the Pt/BaO/Al$_2$O$_3$ sample reduced in H$_2$.

decreased during the experiment. In the cases where the catalyst was sintered at 400 and 550°C before the activity measurements, the activity was about the same. When the sintering temperature was increased to 650°C the activity of the catalyst increased. However, after sintering at 750°C the activity decreased slightly again. What can also be observed in Fig. 9 is that the amount of stored NO$_x$ was about the same for the two lower sintering temperatures, but for 650°C, the amount of stored NO$_x$ decreased, and even more so for a sintering temperature of 750°C. Figure 10 shows the NO oxidation experiment. The activities measured after the two lowest sintering temperatures are about the same. The activity increased slightly when the sintering temperature was increased to 650°C. Further, the results from the experiment for the 750 and 650°C sintering temperature are similar.

3.3. XPS Studies: Pt Oxidation State in Pt/Al$_2$O$_3$ and Pt/BaO/Al$_2$O$_3$ after Different Pretreatments

An example of a survey spectrum is shown in Fig. 11 for the H$_2$-treated Pt/BaO/Al$_2$O$_3$ sample. One can observe Pt peaks at 70–75 eV (Pt 4f), at 316 eV (Pt 4d$_{5/2}$), and at 332 eV (Pt 4d$_{3/2}$). Al shows peaks at 119 (Al 2s) and 74 eV (Al 2p). The latter peak overlaps with the Pt 4f doublet, which often makes analysis of these peaks difficult. In the present case one may note that the Al 2p peak is smaller than the Pt doublet since the Al 2s and 2p peaks are of similar magnitude (37). Also observable are Ba 3d (795 and 780 eV), O 1s (531 eV), and C 1s (285 eV) peaks. The resulting Pt 4f peaks from a more careful analysis are shown in Fig. 12. The position of these peaks and of the Pt 3d$_{5/2}$ peak are given in Table 7. Spectra were taken after pretreatment in H$_2$, NO$_2$, and O$_2$ for Pt/Al$_2$O$_3$ and Pt/BaO/Al$_2$O$_3$. The Pt 3d$_{5/2}$ peak is intrinsically broad but, due to the overlap between Al 2p and Pt 4f, often used for analysis of the oxidation state of Pt in Al-containing samples. The data for

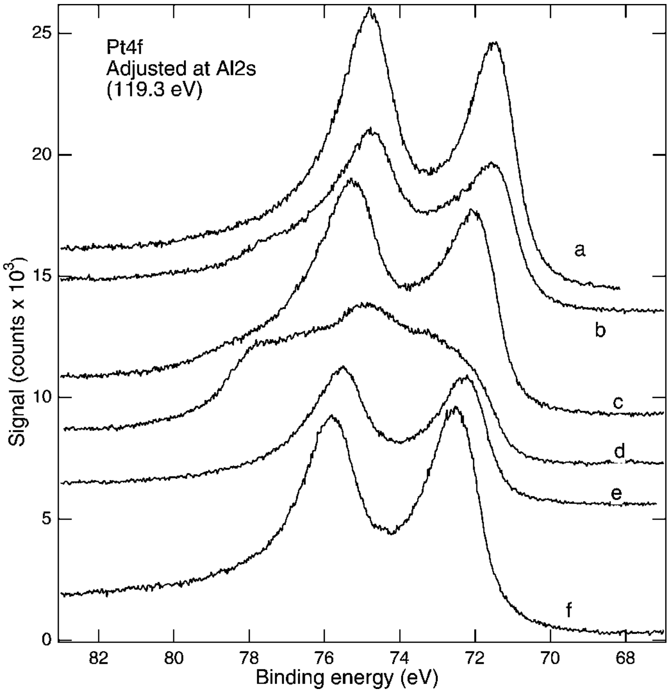

FIG. 12. XPS Pt 4f spectra for different pretreatments: (a) Pt/Al$_2$O$_3$ prereduced in H$_2$, (b) Pt/BaO/Al$_2$O$_3$ prereduced in H$_2$, (c) Pt/Al$_2$O$_3$ pretreated in NO$_2$, (d) Pt/BaO/Al$_2$O$_3$ pretreated in NO$_2$, (e) Pt/Al$_2$O$_3$ preoxidized in O$_2$, and (f) Pt/BaO/Al$_2$O$_3$ preoxidized in O$_2$. The energy scale is adjusted by setting Al 2s at 119.3 eV.

TABLE 7

Experimentally Obtained XPS Peak Positions (eV)

Catalyst	Pretreatment gas	Curve in Fig. 12	Pt $4f_{7/2}$	Pt $4f_{5/2}$	Pt $4d_{5/2}$
Pt/Al_2O_3	H_2	a	71.5	74.8	315.0
$Pt/BaO/Al_2O_3$	H_2	b	71.5	74.7	315.3
Pt/Al_2O_3	NO_2	c	72.1	75.3	315.9
$Pt/BaO/Al_2O_3$	NO_2	d		75.0[a]	317.1
Pt/Al_2O_3	O_2	e	72.3	75.5	316.0
$Pt/BaO/Al_2O_3$	O_2	f	72.6	75.8	316.2

[a] Pt 4f peaks not distinguishable.

this peak in Table 7 show that the peak position is shifted, compared with the Pt^0 value of 314.2 eV obtained for Pt films (21), for the H_2-treated samples. The samples treated in O_2 or NO_2 are shifted even more and the strongest shift is observed for the $Pt/BaO/Al_2O_3$ sample treated in NO_2. In the Pt 4f region, the H_2-treated samples show peaks at 74.8 ($4f_{5/2}$) and 71.5 eV ($4f_{7/2}$) for both Pt/Al_2O_3 and $Pt/BaO/Al_2O_3$. A shift of Pt peaks toward higher binding energies, about 0.5 eV, have been reported when Pt is present on alumina (21, 38, 39). These binding energies thus correlate well with reported values for Pt^0 (21, 40) showing that the reduced samples contain mainly metallic Pt. However, at least for the Ba-containing sample, smaller peaks at higher binding energies are also present. For example, a shoulder can be observed at around 77.7 eV. The NO_2-treated Pt/Al_2O_3 sample shows shifts of both peaks to 75.3 and 72.1 eV, respectively. Further, there is a relatively higher signal between the peaks compared with the spectrum for the H_2-treated sample. The spectrum for the NO_2-treated $Pt/BaO/Al_2O_3$ sample is very different from the H_2-treated case. A main peak at around 75.0 eV can be observed with strong shoulders at around 77.6 and 73.3 eV. The spectrum for the O_2-treated Pt/Al_2O_3 is similar to the NO_2-treated case. The O_2-treated $Pt/BaO/Al_2O_3$ sample shows peaks at 75.8 and 72.6 eV.

As will be discussed below, one interpretation of these shifts is that Pt is oxidized to PtO and PtO_2. According to Kaushik (21), the peaks for PtO in Al_2O_3 should be at 72.4 and 75.6 eV while PtO_2 should show peaks at 74.1 and 77.4 eV. It does thus seem that the O_2-treated $Pt/BaO/Al_2O_3$ sample contains a large amount of PtO while the NO_2-treated sample also contains PtO and a significant amount of PtO_2. Curve fitting was done as described under Experimental and the resulting concentrations of Pt, PtO, and PtO_2 for the six spectra in Fig. 12 are given in Table 8. Figure 13 gives an example of a curve fit for the $Pt/BaO/Al_2O_3$ sample pretreated in NO_2. It should be observed that the fitting of these spectra to six Pt peaks and the Al 2p peak gives a somewhat unclear result. For example, starting values for the positions of the peaks for the three compounds need to be chosen. We have used data for the pure compounds shifted by 0.5 eV due to Pt–Al_2O_3 interaction (21). Thus, the results in Table 8 should only be regarded as indications of the way in which the oxidation state of Pt changes. However, the relative abundance of the three Pt species seems to be fairly consistent between fits that resulted in somewhat different parameter values. From Table 8 one can note that the reduced samples contain a large fraction of Pt^0 while the oxidized samples contain mainly Pt oxides. Pt is oxidized further by NO_2 than O_2 and the presence of BaO increases the oxidation of Pt.

TABLE 8

Relative Abundance of Different Pt Species from Fitting of XPS Data Taken after Pretreatment in H_2, NO_2, or O_2

Catalyst	Pretreatment gas	Curve in Fig. 12	Pt^0 (%)	PtO (%)	PtO_2 (%)
Pt/Al_2O_3	H_2	a	75	16	9
$Pt/BaO/Al_2O_3$	H_2	b	58	27	15
Pt/Al_2O_3	NO_2	c	25	57	18
$Pt/BaO/Al_2O_3$	NO_2	d	7	44	49
Pt/Al_2O_3	O_2	e	28	64	8
$Pt/BaO/Al_2O_3$	O_2	f	20	67	13

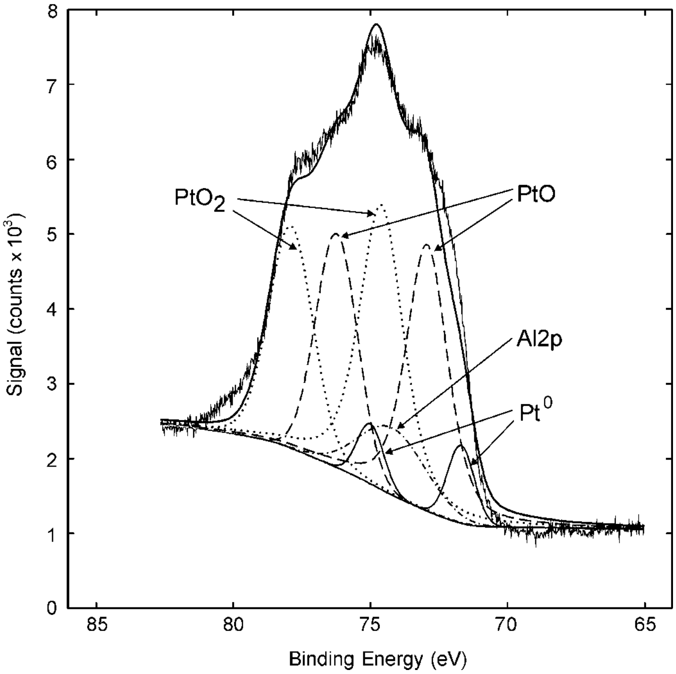

FIG. 13. Curve fit of the XPS Pt 4f spectra for the $Pt/BaO/Al_2O_3$ sample pretreated in NO_2.

4. DISCUSSION

Figure 1 shows the results from a flow reactor experiment with a Pt/Al_2O_3 monolith during a 3-h exposure to NO_2/Ar at 350°C. The concentration of NO decreases gradually during the experiment. Initially the NO_x signal increases and after about 20 min it reaches its a steady-state level. The reason for this slow increase is that there is some initial storage of NO_x on alumina. When an Al_2O_3 catalyst is exposed to NO_2 there is NO formation during the storage process (41) when nitrates are formed. Therefore, during the first 20 min of the NO_2 exposure experiments some of the NO formed originates from the storage process. However, since there is an activity decrease in the catalyst during the whole 3-h exposure, another mechanism to explain the decrease in NO concentration is called for. To facilitate the investigation of the activity decrease it is important to choose temperatures where NO and NO_2 are not in equilibrium after passing over the catalyst. The reason for this is that when the gas components are at equilibrium the activity decrease is difficult to observe, since the active sites are in excess, and even if a substantial fraction of the sites is inactive it may still not influence the conversion. In the NO oxidation experiments, shown in Fig. 3, the catalyst was exposed to $NO/O_2/Ar$ for 180 min at 250 and 300°C. During this time the NO oxidation activity decreased for both temperatures, but the activity decrease was largest at the low temperature (250°C). The temperature dependence of the activity decrease with time during NO_2 dissociation was investigated and the results are given in Fig. 2, which shows the result for NO_2 exposure at 300, 350, and 400°C. The experimental accuracy for observing the deactivation of platinum is best at 350°C for the NO_2 dissociation experiments and therefore this temperature was used for the mechanistic experiments. However, this does not necessarily mean that the deactivation of the catalyst is most rapid at 350°C. At 300°C the dissociation of NO_2 to NO is very slow on metallic platinum. The rate-determining step for this process is the desorption of oxygen from platinum (10) and at 300°C this rate is very low. Due to this low initial NO_2 dissociation activity it cannot be used to study the deactivation. It should also be pointed out that during the first 20 min some of the NO that is formed originates from the NO_x storage on alumina, as described above. Further, at 400°C the activity decreases very slowly, probably because the concentrations are close to equilibrium. The rate of the platinum deactivation cannot easily be compared between exposure to NO_2 and exposure to $NO + O_2$, since we cannot study them at the same temperature. For NO_2 the minimum temperature to study deactivation is about 350°C, due to the slow desorption of oxygen from platinum, and for $NO + O_2$ the maximum temperature is about 250°C, since at higher temperatures the reaction is to close to thermodynamic equilibrium. It is also found that treatment with O_2/Ar alone also deactivates the catalyst. This is shown in an experiment where the Pt/Al_2O_3 catalyst is exposed to NO_2 for 20 min followed by 60 min of O_2 and 10 min of NO_2. The results given in Fig. 6 show that the activity to dissociate NO_2 to NO is decreased also after exposure to oxygen.

The dispersion after increasing sintering temperatures has been investigated with CO-TPD experiments and the results are given in Table 2. We have chosen to present the dispersion as the Pt/CO ratio. There may be some problems with getting an exact absolute value of the dispersion with this method, since there is the risk that some CO desorbs during the Ar flow before the temperature ramp, which would give an underestimation of the dispersion. The dispersion for samples C2 (Pt/Al_2O_3) and C3 ($Pt/BaO/Al_2O_3$) after the pretreatment at 750°C was also measured by hydrogen chemisorption, which, as expected, gives a somewhat higher dispersion. However, the results are in the same range and the CO/Pt ratio clearly shows that the dispersion decreases with increasing sintering temperature. The capacity of platinum to oxidize NO to NO_2 is influenced by the dispersion of the catalyst: When particle size increases, activity also increases (15, 16, 18). Our experimental data also support the previous work. Figure 5 shows that the activity during a temperature ramp increases when the dispersion decreases in spite of the fact that the number of active sites decreases. Further, the dispersion effect on the corresponding NO_2 dissociation to NO shows the same trend: The activity increases when the dispersion decreases, which is shown in Fig. 4.

The support material influences the activity of platinum. According to Yazawa *et al.* (30) the low-temperature activity for propane oxidation is higher for platinum supported on acidic support. Further, Takahashi *et al.* (42) also state that the HC conversion decreases when the alkalinity of the support increases. Since BaO is a material commonly used for NO_x storage catalysts (8) we investigated the difference between Pt supported on Al_2O_3, which is acidic, and on BaO/Al_2O_3, which is alkaline. Figures 5 and 10 show the NO oxidation capacity for Pt/Al_2O_3 and $Pt/BaO/Al_2O_3$, respectively. From these figures it is seen that also the NO oxidation capacity is higher when Pt is supported on Al_2O_3 as opposed to BaO/Al_2O_3. The trend is the same for NO_2 dissociation, which can be seen when comparing Figs. 4 and 9. What should also be mentioned is that for the $Pt/BaO/Al_2O_3$ sample, the NO_x storage is larger on BaO than on Al_2O_3, which results in a larger initial formation of NO due to storage. The Pt/CO ratio for the Pt supported on BaO/Al_2O_3 was about 0.01 for all pretreatment temperatures (400, 550, 650, and 750°C), which is shown in Table 6. The results for the corresponding experiment for Pt/Al_2O_3 are given in Table 2, and in this case the dispersion was much higher, e.g., Pt/CO ratio of 0.07 for a pretreatment temperature of 400°C. This is also supported by previous FTIR measurements, which gave similar result (10). The finding that the dispersion of platinum supported on BaO/Al_2O_3 is so low (1%) may be due to the fact that during the platinum impregnation of the catalyst (in the preparation of the samples) some barium may dissolve. This could result in the possibility that some of the platinum is covered by barium compounds. Further, EDX measurements of a similar powder sample showed a very low platinum signal, which indicates that barium compounds cover some of the platinum. Therefore, the CO-TPD and hydrogen chemisorption experiment for the $Pt/BaO/Al_2O_3$ catalyst should not be used for determining the size of the Pt particles, since we do not know the amount of platinum below barium. Further, it is also possible that the reason that the dispersion did not decrease significantly when the $Pt/BaO/Al_2O_3$ sample was pretreated at high temperatures is that it already was so low that a further decrease was hard to detect.

To investigate the reason for the activity decrease with time of platinum during these reactions the oxidation state of platinum was studied with XPS after different pretreatments. Figure 12 shows the spectra for three different pretreatments: H_2, O_2, and NO_2. The shift for platinum XPS peaks for reduced Pt/Al_2O_3 samples is usually attributed to metal–support interactions (40). The magnitude of this shift has been reported to depend on the Pt particle size. Because of the high Pt loading and the relatively low dispersion measured in the chemisorption experiments, we do not believe that the Pt particles are very small for these samples. However, we still see a shift for the reduced samples. Following the oxidative pretreatments we see the Pt peaks shift, as can be seen in Table 7 and Fig. 12. This shift can in principle have two different causes. One explanation could be that the Pt particles are redispersed during the oxidative treatments. This would give a sample with smaller particles that are more strongly influenced by the $Pt–Al_2O_3$ interaction and thus produce XPS spectra with a stronger shift (38, 40). However, in the paper by Huizinga *et al.* (38), this effect is reported for samples with a higher dispersion than in the present case, and also, the shift is smaller then the ~1 eV observed here. According to Shyu and Otto (40) a mild reduction at 150°C can be used to determine whether metal–support interaction is causing the shift. We have performed such an experiment and find that we have relatively large Pt particles, which are not expected to be strongly shifted because of this effect.

A second possible explanation is that platinum forms oxides (PtO and PtO_2) when treated in O_2 or NO_2 at high temperatures. This should result in shifts of the 3d peak toward higher binding energies, as we observe. For the 4f region one can expect overlapping doublets from the three oxidation states in this case (19, 21). According to Kaushik (21), the shape of the 4f peaks for mixed oxidation states may be a large central peak with pronounced shoulders, similar to what can be observed in Fig. 12, curve d. The 4f region is more suitable for analysis of mixed oxidation states than for the 3d peaks, for which it is difficult to analyze the relative abundance of the three oxidation states since these peaks are so broad. Also note that the Al 2p peak is present in the Pt 4f region (at 74.3 eV). However, when comparing with the size of the Al 2s peak (Fig. 11) it is obvious that it is not the Al 2p peak that is observed as the central maximum in Fig. 12, curve d. Thus, because of (i) the relatively low dispersion, (ii) the relatively large shift, and (iii) the shape of the 4f peaks, we believe that oxidation of Pt takes place in the present experiments. However, we cannot totally exclude the possibility that the oxidative treatments redisperse Pt and cause the observed shift. The shape of the 4f spectra would in that case be connected with the presence of differently sized Pt particles. Curve fitting was performed on the spectra shown in Fig. 12 and the results are given in Table 8. The Pt/Al_2O_3 sample contains a large amount of metallic Pt (75%) after prereduction in H_2. The amount of PtO increases from 16% for pretreatment in H_2 to about 60% in the case of preoxidation with either O_2 or NO_2. The amount of PtO_2 is quite small in all cases for the Pt/Al_2O_3 sample.

Further, three oxygen-TPD experiments were performed with three different exposures of O_2, as shown in Fig. 8. For the low dose of O_2 the oxygen/CO ratio (comparison between O_2- and CO-TPD) was about 1.0 and the Pt sites were covered by, most likely chemisorbed, oxygen, but after a longer exposure (270 min, 8% O_2) the amount of adsorbed oxygen increased substantially, to an oxygen/CO ratio of about 2.4. These experiments support the finding that platinum oxides are formed after long exposure to oxygen. This result is supported both by the XPS measurements that support platinum oxide formation after oxygen exposure and by the flow reactor experiment with the experimental sequence of 20 min of NO_2, 60 min of O_2, 10 min of NO_2, described above. However, as an alternative to oxide formation one may consider that during the long oxygen exposure platinum could redisperse (40), leading to an increasing number of surface Pt sites and thus to an increased amount of oxygen adsorbed. Further, according to Putna *et al.* (43) small platinum particles (2 nm) adsorb oxygen more strongly than larger ones (10 nm) and they concluded that the behavior of 10-nm particles was close to that of Pt(111). To compare with our particles we estimated the diameter from the hydrogen chemisorption according to (44)

$$H/Pt = 0.885/d,$$

which gives 22 nm for the low-dispersion Pt/Al_2O_3 sample (C2). The value for catalyst C1 (Pt/Al_2O_3) which was used in the oxygen-TPD experiments can be estimated based on the fact that the CO/Pt ratio was 1.3 times larger than for C2, which gives a diameter of 17 nm. This value is larger than 10 nm and therefore the platinum particles probably behave similarly to a Pt(111) surface in this respect. Further, low-temperature reduction experiments, which can differ between particulate and dispersed platinum (40), also indicated that catalysts C4 and C5 were mainly in the particulate phase. To conclude, it is not likely that oxygen is adsorbed more strongly after a possible redispersion, since our particles were so large from the beginning (17 nm). Our results show that the deactivation is due to oxygen poisoning. We use the term platinum oxide in this article, but it should be remembered that it could also be strongly chemisorbed oxygen.

The results in Table 8 also show that Pt supported on BaO/Al_2O_3 is much more easily oxidized. When this sample is pretreated with O_2 or NO_2 only small amounts of metallic platinum are present and after the NO_2 exposure as much as 49% of the platinum is in the form of PtO_2. This dramatic change can also easily be observed in Fig. 12, when comparing curves b and d. A realistic theory regarding the influence of the support on the platinum is given by Yoshida *et al.* (24). They state that an acidic support is electrophilic and that the 5d band in platinum donates electron density to the support. Further, electrons are transferred from Pt to oxygen when forming platinum oxide and in the case of an alkaline support there is a higher electron density in Pt, which results in a larger platinum oxide formation (24). This theory agrees well with our experimental results that Pt on BaO, which is alkaline, forms more oxides than Pt supported on Al_2O_3 (which is acidic).

The XPS data show a larger signal for the Pt/Al_2O_3 catalyst compared with that of the $Pt/BaO/Al_2O_3$ catalyst for hydrogen and NO_2 pretreatment. This also supports the fact that there are fewer surface platinum sites on the $Pt/BaO/Al_2O_3$ catalyst, which was seen from CO-TPD measurements. However, for the last experiment with exposure to oxygen the Pt 4f peaks for the Pt/Al_2O_3 sample (Fig. 12) become smaller than the $Pt/BaO/Al_2O_3$ peak. One likely explanation for this is that the Pt particles sintered during the reduction in hydrogen at 500°C that preceded the O_2 treatment (40, 44). The Pt/Al_2O_3 catalyst probably sinters more easily than $Pt/BaO/Al_2O_3$, which was seen from the CO-TPD experiments. Further, it is possible that the XPS signal is influenced by nitrate species on the support. However, the deactivation seen in the flow reactor experiments occurs long after the catalysts have been saturated with NO_x, which implies that the deactivation is not due to nitrate formation. Further, an activation decrease is also seen when exposing the catalyst to only O_2/Ar (Fig. 6).

To conclude, the decrease in activity that has been seen in flow reactor experiments most probably comes from the fact that platinum oxides are formed and that these oxides are less active than metallic platinum. Yazawa *et al.* (30) investigated another system, propane combustion on platinum supported on SiO_2–Al_2O_3 or ZrO_2. They concluded that platinum oxide was formed during oxygen exposure and that oxide had a lower activity. This study supports the theory that during NO_2 exposure in our experiments the platinum is slowly oxidized and therefore loses activity.

The regeneration of the samples deactivated in NO_2 exposure was investigated (Fig. 7). During the first 60 min of NO_2 exposure of the Pt/Al_2O_3 catalyst at 350°C the conversion of NO_2 to NO gradually decreases. Then the catalyst is cooled to 90°C in NO_2/Ar and at this temperature exposed to Ar for 60 min, followed by an increase in temperature back to 350°C with a NO_2 exposure of the catalyst. After this treatment the catalyst is completely inactive. This is probably due to the fact that the coverage of oxygen on the surface has increased even more, either as chemisorbed oxygen or as oxides. At 350°C the desorption of oxygen is quite slow compared to that at higher temperatures, which can be seen in Fig. 8. However, since during the first 60 min of NO_2 exposure there was substantial NO_2 dissociation, it must mean that there is a quite large amount of chemisorbed oxygen that desorbs at this temperature. This speaks against the suggestion that it is mostly chemisorbed oxygen that totally inhibits the surface. After flushing the catalyst with Ar the sample is again exposed to NO_2 and now it regains some activity. The reason may be that loosely bound oxygen desorbs. The activity for NO oxidation is now tested and it shows that the activity is quite high and that during the NO and O_2 exposure the activity increases. This may be interpreted as NO acting as a reducing agent and thus the amount of oxygen on the surface is decreased. After the $NO + O_2$ exposure the inlet gas is changed (after flushing with Ar) to NO_2 again and now the catalyst can dissociate a substantial amount of NO_2 to NO. Thus it is obvious that the $NO + O_2$ exposure regenerated the catalyst. However, the activity is not as high as it was initially.

As described above, large particles are more active than small particles for NO_2 dissociation and NO oxidation, which is seen in Figs. 4 and 5. According to Altman and Gorte (45) small Pt particles contain a higher concentration of low-coordinated sites compared to large particles, which expose more of the closely packed (111) sites. Further, small particles becomes oxidized more easily (23, 34). It is therefore possible that the reason for the high activity of the large platinum particles is that the (111) surfaces may be more difficult to oxidize than more-open surfaces. To conclude, the reason for the high activity of large platinum particles for NO oxidation may be that they are more stable toward platinum oxide formation.

These results have implications for the NO_x storage concept with BaO-containing catalysts. It has previously been shown in literature that the NO oxidation activity is lower for Pt supported on BaO/Al_2O_3 than on Al_2O_3 (10) and in this study we have shown that $Pt/BaO/Al_2O_3$ forms more platinum oxides than does Pt/Al_2O_3 and that the platinum oxide is less active. On the basis of these findings we suggest that one reason for the fact that Pt supported on BaO/Al_2O_3 is less active for NO oxidation (and also for HC oxidation) than Pt supported on Al_2O_3 may be that Pt on BaO/Al_2O_3 forms more platinum oxides. It may therefore be beneficial to modify the catalyst for decreasing the amount of oxides, e.g., by making an alloy with platinum or replacing platinum with another metal. Alternatively, use of storage material that does not have this negative effect on platinum may give improved performance.

5. CONCLUSIONS

In this paper, we present an experimental investigation of the decrease in activity with time for NO oxidation and NO_2 dissociation. Further, the effect of the platinum dispersion on the activity is also investigated. The catalysts used are Pt/Al_2O_3 and $Pt/BaO/Al_2O_3$. The main conclusions are summarized below.

Pt/Al_2O_3

- During NO_2/Ar exposure (at 350°C) the activity of platinum in dissociating NO_2 to NO decreased during the experiments. Even after 3 h no steady-state level had been reached.
- During NO oxidation ($NO + O_2$ exposure) the activity also decreased during reaction. This was seen at 250 and 300°C. Higher temperatures could not be used since the concentration then reached equilibrium.
- Experiments also showed that even O_2/Ar was able to deactivate the catalyst.
- One probable interpretation of the XPS experiments is that platinum oxide was formed when exposing the catalyst to O_2 or NO_2 and we therefore conclude that the activity decrease with time seen in the experiments is likely due to formation of platinum oxide, which is less active than metallic platinum. Further O_2- and CO-TPD experiments on Pt gave an oxygen/CO ratio well above 1, which would imply that there is a combination of PtO and PtO_2 on the surface, which also the XPS spectra indicated.
- When the dispersion of platinum decreased, the activity of platinum for NO oxidation and NO_2 dissociation increased. The reason for this may be that the small particles formed more platinum oxide, which is less active.

$Pt/BaO/Al_2O_3$

- Platinum supported on BaO/Al_2O_3 is less active than platinum supported on Al_2O_3, both for NO oxidation and for NO_2 dissociation.
- From XPS measurements we suggest that there was much more PtO_2 formed on $Pt/BaO/Al_2O_3$ than on Pt/Al_2O_3. This may explain the low activity on $Pt/BaO/Al_2O_3$. A possible explanation for the lower platinum oxide formation on platinum supported on Al_2O_3 may be that since Al_2O_3 is acidic it is more electrophilic and the 5d band in platinum donates electron density to the support. Further, electrons are transferred from Pt to oxygen when platinum oxide is formed and in the case of an acidic support there is a lower electron density in Pt, which gives less platinum oxide. BaO, on the other hand, is alkaline and influences platinum in the opposite way; thus more platinum oxide is formed.

ACKNOWLEDGMENTS

The work in this paper was performed at the Competence Centre for Catalysis, which is financially supported by the Swedish National Energy Administration and the member companies: AB Volvo, Johnson Matthey–CSD, Saab Automobile AB, Perstorp AB, MTC AB, Eka Chemicals, and the Swedish Space Corporation.

REFERENCES

1. Houghton, J., “Global Warming—The Complete Briefing.” Cambridge Univ. Press, Cambridge, U.K., 1997.
2. Fritz, A., and Pitchon, V., *Appl. Catal. B* **13**, 1 (1997).
3. Burch, R., and Watling, T. C., *Stud. Surf. Sci.* **116**, 199 (1998).
4. Burch, R., Fornasiero, P., and Watling, T. C., *J. Catal.* **176**, 204 (1998).
5. Acke, F., and Skoglundh, M., *Appl. Catal. B* **22**, L1 (1999).
6. Miyoshi, N., Matsumoto, S., Katoh, K., Tanaka, T., Harada, J., Takahashi, N., Yokota, K., Sugiura, M., and Kasahara, K., *SAE Tech. Pap. Ser.* **950809**, 120 (1995).
7. Bögner, W., Krämer, M., Krutzsch, B., Pischinger, S., Voigtländer, D., Wenninger, G., Wirbeleit, F., Brogan, M. S., Brisley, R. J., and Webster, D. E., *Appl. Catal. B* **7**, 153 (1995).
8. Fridell, E., Skoglundh, M., Westerberg, B., Johansson, S., and Smedler, G., *J. Catal.* **183**, 196 (1999).
9. Fridell, E., Persson, H., Westerberg, B., Olsson, L., and Skoglundh, M., *Catal. Lett.* **66**, 71 (2000).
10. Olsson, L., Persson, H., Fridell, E., Skoglundh, M., and Andersson, B., *J. Phys. Chem. B* **105**, 6895 (2001).
11. Matsumoto, S., Ikeda, Y., Suzuki, H., Ogai, M., and Miyoshi, N., *Appl. Catal. B* **25**, 115 (2000).
12. Schmitz, P. J., and Baird, R. J., *J. Phys. Chem. B* **106**, 4172 (2002).
13. Broqvist, P., Panas, I., Fridell, E., and Persson, H., *J. Phys. Chem. B* **106**, 137 (2002).
14. Olsson, L., Westerberg, B., Persson, H., Fridell, E., Skoglundh, M., and Andersson, B., *J. Phys. Chem. B* **103**, 10433 (1999).
15. Lee, J.-H., and Kung, H. H., *Catal. Lett.* **51**, 1 (1998).
16. Xue, E., Seshan, K., and Ross, J. R. H., *Appl. Catal. B* **11**, 65 (1996).
17. Jayat, F., Lembacher, C., Schubert, U., and Martens, J. A., *Appl. Catal. B* **21**, 221 (1999).
18. Denton, P., Giroir-Fendler, A., Praliaud, H., and Primet, M., *J. Catal.* **189**, 410 (2000).
19. Pitchon, V., and Fritz, A., *J. Catal.* **186**, 64 (1999).
20. Jung, M.-C., Kim, H.-D., Han, M., Jo, W., and Kim, D. C., *Jpn. J. Appl. Phys.* **38**(8), 4872 (1999).
21. Kaushik, V. K., *Z. Phys. Chem.* **173**, 105 (1991).
22. Hwang, C.-P., and Yeh, C.-T., *J. Catal.* **182**, 48 (1999).
23. Borgna, A., Le Normand, F., Garetto, T., Apesteguia, C. R., and Moraweck, B., *Catal. Lett.* **13**, 175 (1992).
24. Yoshida, H., Yazawa, Y., Takagi, N., Satsuma, A., Tanaka, T., Yoshida, S., and Hattori, T., *J. Synchrotron Rad.* **6**, 471 (1999).
25. Hwang, C.-P., and Yeh, C.-T., *J. Mol. Catal. A* **112**, 295 (1996).
26. Wang, C.-B., and Yeh, C.-T., *J. Catal.* **178**, 450 (1998).
27. Wang, C.-B., and Yeh, C.-T., *Appl. Catal. A* **209**, 1 (2001).
28. Niehus, H., and Comsa, G., *Surf. Sci.* **93**, L147 (1980).
29. Saliba, N. A., Tsai, Y.-L., Panja, C., and Koel, B. E., *Surf. Sci.* **419**, 79 (1999).
30. Yazawa, Y., Kagi, N., Komai, S., Satsuma, A., Murakami, Y., and Hattori, T., *Catal. Lett.* **72**, 157 (2001).
31. Dicke, J., Rotermund, H.-H., and Lauterbach, J., *Surf. Sci.* **454–456**, 352 (2000).
32. von Oertzen, A., Mikhailov, A., Rotermund, H.-H., and Ertl, G., *Surf. Sci.* **350**, 259 (1996).
33. Lauterbach, J., Asakura, K., and Rotermund, H. H., *Surf. Sci.* **313**, 52 (1994).

34. Hartmann, N., Imbihl, R., and Vogel, W., *Catal. Lett.* **28**, 373 (1994).
35. Skoglundh, M., Johansson, H., Löwendahl, L., Jansson, K., Dahl, L., and Hirschauer, B., *Appl. Catal. B* **7**, 299 (1996).
36. Zslodos, Z., Garin, F., Hilaire, L., and Guczi, L., *Catal. Lett.* **33**, 39 (1995).
37. Moulder, J. F., Stickle, W. F., Sobol, P. E., and Bomben, K. D., "Handbook of X-Ray Photoelectron Spectroscopy." Perkin–Elmer, Palo Alto, CA, 1992.
38. Huizinga, T., van't Blik, H. F. J., Vis, J. C., and Prins, R., *Surf. Sci.* **135**, 580 (1983).
39. Talo, A., Lahtinen, J., and Hautojärvi, P., *Appl. Catal. B* **5**, 221 (1995).
40. Shyu, J. Z., and Otto, K., *Appl. Surf. Sci.* **32**, 246 (1988).
41. Underwood, G. M., Miller, T. M., and Grassian, V. H., *J. Phys. Chem. A* **103**, 6184 (1999).
42. Takahashi, N., Shinjoh, H., Iijima, T., Suzuki, T., Yamazaki, K., Yokota, K., Suzuki, H., Miyoshi, N., Matsumoto, S., Tanizawa, T., Tanaka, T., Tateishi, S., and Kasahara, K., *Catal. Today* **27**, 63 (1996).
43. Putna, E. S., Vohs, J. M., and Gorte, R. J., *Surf. Sci.* **391**, L1178 (1997).
44. Dautzenberg, F. M., and Wolters, H. B. M., *J. Catal.* **51**, 26 (1978).
45. Altman, E. I., and Gorte, R. J., *Surf. Sci.* **195**, 392 (1988).